

## Effects of organic film morphology on the formation of Rb clusters on surface coatings in alkali metal vapor cells

D. M. Rampulla,<sup>1</sup> N. Oncel,<sup>1</sup> E. Abelev,<sup>1</sup> Y. W. Yi,<sup>2</sup> S. Knappe,<sup>3</sup> and S. L. Bernasek<sup>1,a)</sup>

<sup>1</sup>*Department of Chemistry, Princeton University, Princeton, New Jersey 08544, USA*

<sup>2</sup>*Department of Physics and Liquid Crystal Materials Research Center, University of Colorado, Boulder, Colorado 80309, USA*

<sup>3</sup>*Time and Frequency Division, National Institute of Standards and Technology, Boulder, Colorado 80305, USA*

(Received 15 August 2008; accepted 31 December 2008; published online 29 January 2009)

Surface relaxation rates differ for spin-polarized alkali atoms interacting with monolayer or bilayer octadecyltrichlorosilane (OTS) coatings. The morphology and composition of Rb vapor-exposed films of OTS have been studied with atomic force microscopy (AFM) and x-ray photoelectron spectroscopy (XPS). On OTS monolayers, numerous small (<500 nm wide) Rb containing islands nucleate at the boundaries of the  $\sim 1-2 \mu\text{m}$  wide organic domains. On OTS bilayers, singular large ( $\sim 3 \mu\text{m}$  wide) Rb containing islands were found. Alkali island formation mediated by surface structure could affect the antirelaxation behavior of organic coatings used in atomic magnetometer cells. © 2009 American Institute of Physics. [DOI: 10.1063/1.3073711]

Coated alkali vapor cells have found use in atomic magnetometers, atomic clocks, and magneto-optical traps.<sup>1-8</sup> In most experiments, spin-exchange and spin-destruction collisions among alkali atoms occur less frequently than wall collisions; therefore, alkali-wall interactions can completely dictate atomic spin-polarization lifetimes. Spin-polarization lifetimes of alkali atom vapors have been increased through the use of antirelaxation surface coatings.<sup>9,10</sup>

Currently, paraffin is the most effective antirelaxation coating, and it has been shown to be able to allow an alkali atom to collide up to 10 000 times before spin-depolarization. Additionally, the use of octadecyltrichlorosilane (OTS) (an 18 carbon alkyl trichlorosilane) to coat vapor cells has been shown to allow an alkali atom to collide up to 2000 times before depolarization,<sup>11</sup> based on  $T_1$  relaxation time. Recently, relaxation times of spin-polarized K atoms in the presence of OTS monolayers and bilayers were measured; this comparison showed that an OTS bilayer is capable of sustaining a relaxation time five times larger than that found by use of an OTS monolayer,<sup>1</sup> again based on measures of  $T_1$  relaxation time. In this work, the microscopic character of Rb-exposed OTS monolayer and bilayer coatings is examined, relative to the effectiveness of these films as antirelaxation coatings for spin-polarized devices. No previous morphological studies of Rb exposed self-assembled organic layers have been carried out, nor have these films been examined by x-ray photoelectron spectroscopy (XPS) to determine film composition or chemical state of the deposited alkali metal. Winograd and co-workers<sup>12-14</sup> have examined the deposition of K, Au, Mg, and Ti atoms on self-assembled alkanethiol layers. Using time of flight secondary ion mass spectrometry, they obtained evidence for metal atom penetration into the organic layer, along with reaction with the organic coating under some conditions.

OTS monolayer films on silica substrates were grown at the University of Colorado in Boulder by a procedure de-

tailed in Ref. 15. The methods described in this reference were applied to ensure that the coatings are indeed monolayers. Bilayer OTS films were grown on  $\text{SiO}_2/\text{Si}$  substrates at Princeton by use of a procedure that has been previously described.<sup>1</sup> OTS monolayers and bilayers were sealed into evacuated glass bulbs along with Rb metal. The entire bulb was heated to 120 °C for 24 h to expose the OTS coatings to Rb vapor, as done in actual atomic resonance cells. After the 24 h period of Rb exposure, the glass bulb was kept at 120 °C, except for a small spot that was cooled to room temperature. This cold spot was used to trap excess unreacted Rb atoms that evaporate from the warm OTS surfaces. Rb atoms were trapped for a period of 12 h. Once cooled to room temperature, the glass bulbs were opened in a glove box, and the OTS samples removed for XPS and atomic force microscopy (AFM) studies. XP spectra of OTS monolayers were collected using a VG Scientific ESCALAB2 spectrometer with Al  $K\alpha$  radiation ( $h\nu=1486.6 \text{ eV}$ ). XP spectra of OTS bilayers were collected using a SPECS Phoibos 150 hemispherical energy analyzer with a monochromated Al  $K\alpha$  source. The clean OTS monolayer and bilayer films had identical features, regardless of the XP spectrometer used. Curve fitting of the core-level XP lines was carried out using CASAXPS software with a Gaussian-Lorentzian product function and a nonlinear Shirley background subtraction. AFM images were recorded under ambient conditions using a Digital Instruments Nanoscope IIIa.

Figure 1 shows XP spectra of Rb 3*d*, Si 2*p*, and O 1*s* peaks for a Rb-exposed (top row) and a clean (bottom row) OTS monolayer. The OTS bilayer data (not shown) are essentially identical. After Rb exposure, Rb 3*d* peaks are present on the OTS monolayer sample. Additionally, in the Rb-exposed sample a secondary peak with low binding energy appears in both the Si 2*p* and O 1*s* spectra. The O 1*s* spectrum obtained from the Rb-exposed sample is resolved into two components; the primary peak was located at 532.4 eV and attributed to oxygen present in the  $\text{SiO}_2$  substrate and OTS film and the secondary peak was located at a lower binding energy (529.7 eV). Two components were also re-

<sup>a)</sup>Author to whom correspondence should be addressed. Electronic mail: sberna@princeton.edu.

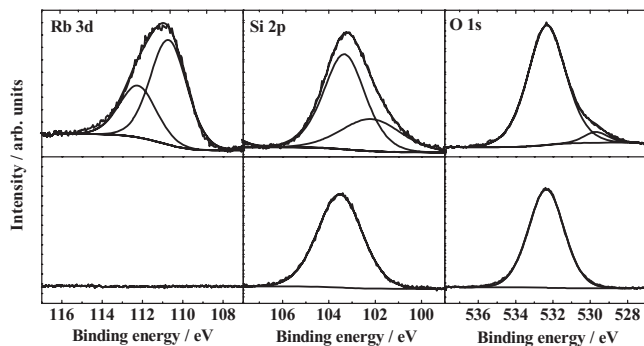


FIG. 1. XPS spectra of Rb  $3d$ , Si  $2p$ , and O  $1s$  core levels for a clean OTS monolayer (lower curves) and a Rb-exposed OTS monolayer (upper curves). The O  $1s$  spectrum is resolved into two components; a primary peak at 532.4 eV attributed to oxygen originally in the  $\text{SiO}_2$  substrate and OTS film, and a secondary peak at 529.7 eV attributed to O atoms reacted with Rb. The Si  $2p$  spectrum is resolved into two components; a primary peak 103.3 eV attributed to Si in the  $\text{SiO}_2$  substrate and OTS film originally, and a secondary peak at 102.1 eV attributed to Si atoms reacted with Rb.

solved in the Si  $2p$  spectrum. The primary peak in the Si  $2p$  spectrum was located at a binding energy of 103.3 eV, which is attributed to Si present in the  $\text{SiO}_2$  substrate and OTS film. The secondary peak in the Si  $2p$  spectra was located at a lower binding energy (102.1 eV). The secondary peaks at lower binding energies in the Si  $2p$  and O  $1s$  spectra are attributed to a change in the chemical environment surrounding some of the Si and O atoms present in the substrate and/or film after Rb exposure. As discussed in Camparo *et al.*<sup>16</sup> the likely product formed during exposure of the OTS layer to Rb is a metal silanolate ( $R\text{-Si-O-M}$ , where  $R$  is an alkyl moiety, and  $M$  is Rb in this case). The possibility exists that there are multiple reaction products, but it is evident that Si and O in both the monolayer and bilayer are susceptible to Rb attack.

The Rb distribution within the OTS bilayer was studied by angle-resolved XPS (ARXPS). High-resolution scans of Rb  $3d$  and Si  $2p$  peaks were acquired at angles of 90°, 50°, 30°, and 20° between the sample surface plane and the entrance to the electron energy analyzer. As shown in Fig. 2, the ratio of silicon to rubidium decreases as the angles become smaller (more surface sensitive), indicating that Rb is located within the film, mostly near the surface. Based on the presence of secondary peaks in the standard XPS spectrum and the presence of Rb within the bilayer film as suggested by ARXPS, data indicate that some O and Si must also be present in the middle of the film to accommodate the Rb bonding seen in XPS.

Attenuation of the Si and O signal was used to verify the bilayer structure of the OTS film on the Si/ $\text{SiO}_2$  sample. The attenuation of substrate spectral features in the presence of a film of thickness  $d$  is given by the relationship

$$I_d = I_o \exp(-d/\lambda \sin \theta), \quad (1)$$

where  $I_o$  and  $I_d$  are, respectively, the spectral signals before and after deposition of a film.  $\lambda$  is the inelastic mean free path (IMFP) and  $\theta$  is the angle between the sample surface and the photoelectron analyzer. It has been reported by Labinis *et al.*<sup>17</sup> that the IMFP of an electron in a hydrocarbon film is proportional to its kinetic energy (where the kinetic energy is between 500–1500 eV), according to Eq. (2),

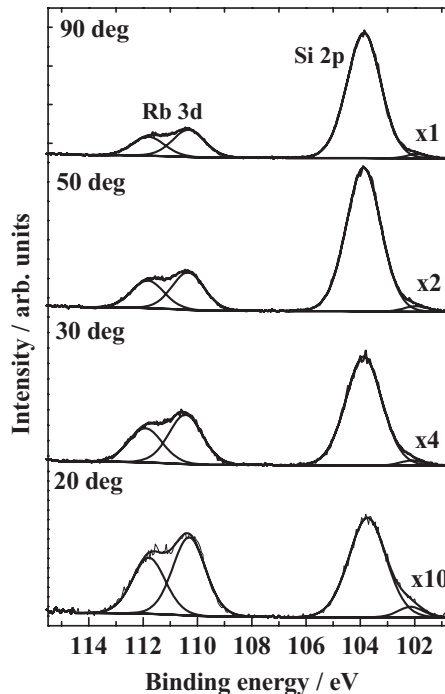


FIG. 2. Angle-resolved XPS spectra of Rb  $3d$  and Si  $2p$  core levels for a Rb-exposed OTS bilayer. The angle between the sample surface and photoelectron analyzer is given in each frame. The Si  $2p$  peaks are as described in Fig. 1. There are two Rb  $3d$  peaks due to spin-orbit splitting.

$$\lambda(\text{\AA}) = 9.0 + [0.022 \times KE \text{ (eV)}] \quad (2)$$

KE is the kinetic energy of the photoelectron. For the Si  $2p$  photoelectron this gives an IMFP of 39.4 Å in the OTS layer, thus yielding a layer thickness of 4.9 nm, which is similar to twice the length of the OTS molecule (4.5 nm), suggesting bilayer formation. The O  $1s$  photoelectron IMFP is 30 Å, thus yielding a layer thickness of 4.5 nm, again consistent with the thickness of a bilayer. Similar calculations from the secondary XPS peaks revealed that Si bonded to Rb is located at an average depth of 2.5 nm from the surface, and O bonded to Rb is located at an average depth of 3.3 nm from the surface. Calculations using the Rb  $3d$  signal reveal that Rb is located at an average depth of 2.4 nm within the OTS bilayer. These average depths suggest a distribution of Rb containing species distributed through the organic layer not localized at the outer surface nor at the OTS-silicon interface.

Following XPS studies, AFM was used to image the morphology of the OTS films after Rb exposure. Figure 3(a) is a  $5 \times 5 \mu\text{m}^2$  height image of an OTS monolayer after Rb exposure. The surface suggests micrometer-wide organic do-

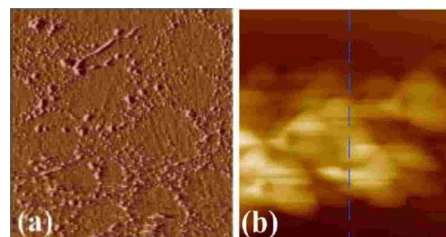


FIG. 3. (Color online) (a) is a  $5 \times 5 \mu\text{m}^2$  height image of a Rb-exposed OTS monolayer measured with an AFM. The protrusions are Rb containing clusters. (b) is a  $5 \times 5 \mu\text{m}^2$  height image of a Rb-exposed OTS bilayer measured with an AFM.

mains surrounded by numerous Rb containing islands. The diameter and the height of these islands are less than 500 and about 40 nm, respectively. The existence of domain boundaries surrounded by Rb containing islands might be expected, since OTS monolayers form dense domains ( $\sim 1 \mu\text{m}$  wide) surrounded by grain boundaries, which are packing defects.<sup>18</sup> Apparently, upon exposure to Rb, these boundaries act as Rb nucleation sites, while leaving the well-formed organic crystallites undisturbed.

On the other hand, Rb containing species on the OTS bilayer have a tendency to form widely separated large islands. In the image shown in Fig. 3(b), the width of the island is  $\sim 3 \mu\text{m}$ . Subsequent imaging of the same island revealed that the length of the island is greater than  $10 \mu\text{m}$ . Since the OTS bilayer film is not grown as an ordered film, it is likely that an amorphous surface anchored to the substrate is formed. Amorphous structures are full of packing defects at the atomic scale, but they do not propagate in a regular fashion to near-micrometer dimensions like a grain boundary. Therefore, these comparably small defects spread around the film may not be large enough to initiate the formation of stable Rb containing islands; instead, Rb species on such a surface may diffuse and lead to the formation of the observed larger islands.

In summary, AFM on Rb-exposed OTS monolayers shows that Rb forms small islands at the grain boundaries. XPS on this sample clearly indicates that some of the Rb atoms diffuse into the film and bond to underlying Si and O. These results are in agreement with the diffusion of metal atoms through self-assembled monolayers, which has been previously studied.<sup>19,20</sup> ARXPS on Rb-exposed OTS bilayers show that Rb atoms also penetrate this film and react with Si and O. However, in contrast to the monolayer, on bilayer OTS films Rb species form large well separated islands. The observed differences in the size and distribution of Rb containing islands between OTS monolayer and bilayer films suggest that the defects on the films have a strong influence on island formation, and such a difference may be responsible for the variations observed for the surface relaxation rates of coatings within atomic resonance cells. However, the

mechanism for this effect on spin relaxation times is not yet understood.

This work was supported by an Office of Naval Research MURI Grant No. N00014-05-1-0406. The authors thank Scott Seltzer, Joe Dennes, and Hugh Robinson for helpful discussions and Hugh Robinson for the preparation of the vapor cells.

- <sup>1</sup>S. J. Seltzer, D. M. Rampulla, S. Rivillon-Amy, Y. J. Chabal, S. L. Bernasek, and M. V. Romalis, *J. Appl. Phys.* **104**, 103116 (2008).
- <sup>2</sup>M. V. Balabas, D. Budker, J. Kitching, P. D. D. Schwindt, and J. E. Stalnaker, *J. Opt. Soc. Am. B* **23**, 1001 (2006).
- <sup>3</sup>M. P. Ledbetter, V. M. Acosta, S. M. Rochester, D. Budker, S. Pustelny, and V. V. Yashchuk, *Phys. Rev. A* **75**, 023405 (2007).
- <sup>4</sup>S. Groeger, A. S. Pazgalev, and A. Weis, *Appl. Phys. B: Lasers Opt.* **80**, 645 (2005).
- <sup>5</sup>J. S. Guzman, A. Wojciechowski, J. E. Stalnaker, K. Tsigurtkin, V. V. Yashchuk, and D. Budker, *Phys. Rev. A* **74**, 053415 (2006).
- <sup>6</sup>D. Budker, L. Hollberg, D. F. Kimball, J. Kitching, S. Pustelny, and V. V. Yashchuk, *Phys. Rev. A* **71**, 012903 (2005).
- <sup>7</sup>Z.-T. Lu, K. L. Corwin, K. R. Vogel, C. E. Wieman, T. P. Dinneen, J. Madi, and H. Gould, *Phys. Rev. Lett.* **79**, 994 (1997).
- <sup>8</sup>M. Stephens, R. Rhodes, and C. Wieman, *J. Appl. Phys.* **76**, 3479 (1994).
- <sup>9</sup>H. Robinson, E. Ensberg, and H. Dehmelt, *Bull. Am. Phys. Soc.* **3**, 9 (1958).
- <sup>10</sup>M. A. Bouchiat and J. Brossel, *Phys. Rev.* **147**, 41 (1966).
- <sup>11</sup>S. J. Seltzer, P. J. Meares, and M. V. Romalis, *Phys. Rev. A* **75**, 051407 (2007).
- <sup>12</sup>Z. Zhu, D. L. Allara, and N. Winograd, *Appl. Surf. Sci.* **252**, 6686 (2006).
- <sup>13</sup>Z. Zhu, T. A. Daniel, M. Maitani, O. M. Cabarcos, D. L. Allara, and N. Winograd, *J. Am. Chem. Soc.* **128**, 13710 (2006).
- <sup>14</sup>A. V. Walker, T. B. Tighe, O. Cabarcos, B. C. Haynie, D. L. Allara, and N. Winograd, *J. Phys. Chem. C* **111**, 765 (2007).
- <sup>15</sup>Y. W. Yi, H. G. Robinson, S. Knappe, J. E. MacLennan, C. D. Jones, C. Zhu, N. A. Clark, and J. Kitching, *J. Appl. Phys.* **104**, 023534 (2008).
- <sup>16</sup>J. C. Camparo, R. P. Frueholz, and B. Jadaszliwer, *J. Appl. Phys.* **62**, 676 (1987).
- <sup>17</sup>P. E. Laibinis, C. D. Bain, and G. M. Whitesides, *J. Phys. Chem.* **95**, 7017 (1991).
- <sup>18</sup>R. Bautista, N. Hartmann, and E. Hasselbrink, *Langmuir* **19**, 6590 (2003).
- <sup>19</sup>A. V. Walker, T. B. Tighe, O. M. Cabarcos, M. D. Reinard, B. C. Haynie, S. Uppili, N. Winograd, and D. L. Allara, *J. Am. Chem. Soc.* **126**, 3954 (2004).
- <sup>20</sup>T. Ohgi, H. Y. Sheng, and H. Nejo, *Appl. Surf. Sci.* **130**, 919 (1998).